

PAPER

Large Rabi splitting in InGaN quantum wells microcavity at room temperature

To cite this article: JinZhao Wu *et al* 2019 *Mater. Res. Express* **6** 076204

View the [article online](#) for updates and enhancements.



IOP | ebooks™

Bringing you innovative digital publishing with leading voices to create your essential collection of books in STEM research.

Start exploring the collection - download the first chapter of every title for free.

Materials Research Express



PAPER

Large Rabi splitting in InGaN quantum wells microcavity at room temperature

RECEIVED
6 March 2019

REVISED
8 April 2019

ACCEPTED FOR PUBLICATION
16 April 2019

PUBLISHED
24 April 2019

JinZhao Wu, XiaoLing Shi, Hao Long¹ , Lan Chen, LeiYing Ying, ZhiWei Zheng and BaoPing Zhang¹

Department of Electronic Engineering, Optoelectronics Engineering Research Center, School of Electronic Science and Engineering (National Model Microelectronics College), Xiamen University, Xiamen 361005, People's Republic of China

¹ Authors to whom any correspondence should be addressed.

E-mail: longhao@xmu.edu.cn and bzhang@xmu.edu.cn

Keywords: strong coupling, exciton polariton, large splitting, InGaN quantum wells, microcavity

Abstract

Room-temperature luminescence of exciton polaritons was observed from InGaN/GaN quantum wells (QWs) sandwiched in Fabry–Perot (FP) microcavity (MC). Angle resolved photoluminescence measurements revealed unambiguous anti-crossing behavior, indicating strong coupling between excitons and photons. The Rabi splitting value varied from 40 meV–130 meV, depending on the excitation power, which was larger than previous publications. This large Rabi splitting value was ascribed to our high MC quality factor ($Q > 3000$) and large oscillator strength induced by coupled QWs structure. The sensitive dependence of the Rabi splitting in InGaN QWs on excitation power indicates that exciton-exciton scattering mechanism plays an important role in exciton–photon coupling.

Semiconductor MC in the strong light–matter coupling region has generated significant impact over the past few decades [1]. A large number of experiments have been performed to study the properties of photons and excitons [2, 3]. When the excitons interact with cavity photons at resonance frequencies, half-matter/half-light quasi-particles known as ‘cavity polaritons’ were produced with an anti-crossing behavior. The exciton polaritons with lower polariton branch (LPB) and upper polariton branch (UPB), were first demonstrated in the angle resolved photoluminescence (PL) experiments by Houdre in 1994 [4]. Exciton polaritons have much lighter effective mass (typically four orders of magnitude smaller than exciton) and tunable energy momentum dispersion. These unique properties made the exciton polaritons been widely adopted in studying cavity quantum electrodynamics, such as Bose–Einstein condensates (BECs) and other fundamental physics [5, 6]. BECs of cavity polariton have received much attention recently, because of their relatively high condensation temperatures [7]. Furthermore, exciton polaritons are also promising for ultra-low threshold laser and parametric amplification [8–11].

Most of the studies on exciton polaritons in planar MC were conducted at relatively low temperatures and in material systems such as GaAs and CdTe [12–15]. So far, the electrically injected cavity polariton based on GaAs cavity has been reported [16, 17]. Moreover, the polaritonic nonlinearities has been observed under electrical injection in GaAs cavity at cryogenic temperature [18, 19]. However, it was hard to achieve the polariton lasing at room temperature due to the small exciton binding energy in GaAs and CdTe systems. When temperature increases, strong coupling disappears because thermal broadening of the exciton resonance exceeds exciton’s binding energy in the GaAs and CdTe [13].

It is noted that, GaN-based semiconductor MC is considered to be a good candidate for studying the exciton polaritons at room temperature due to the following: (1) GaN-based semiconductors have relatively large exciton binding energy (26 meV for bulk GaN, ~46 meV for QWs) and large exciton oscillator strength [13], which satisfied the prerequisite for the strong coupling and room temperature exciton polariton [20, 21]. (2) GaN-based semiconductors have fast relaxation rate, which can effectively suppress the polariton bottleneck effect to benefit polaritons’ condensation [22]. Several research groups have reported the exciton polaritons in bulk GaN material due to their simple structure and good optical properties [23, 24]. In addition, room

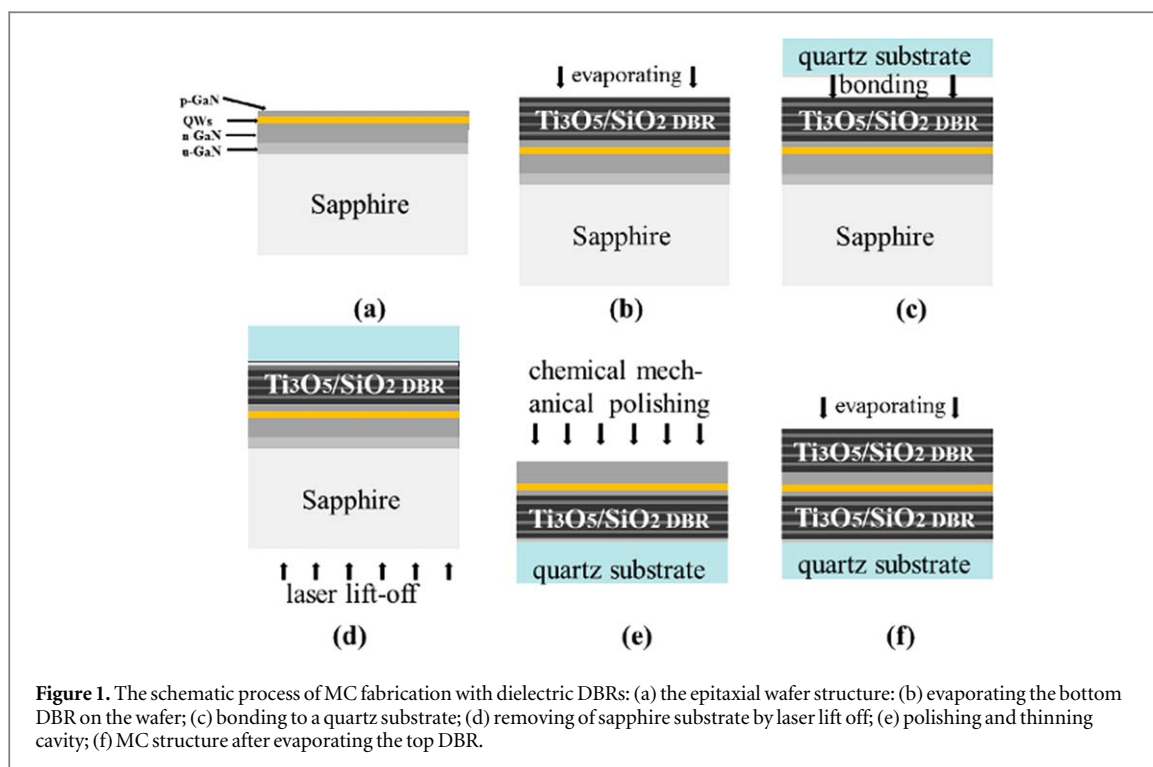


Figure 1. The schematic process of MC fabrication with dielectric DBRs: (a) the epitaxial wafer structure; (b) evaporating the bottom DBR on the wafer; (c) bonding to a quartz substrate; (d) removing of sapphire substrate by laser lift off; (e) polishing and thinning cavity; (f) MC structure after evaporating the top DBR.

temperature polariton lasing was achieved in bulk GaN and GaN nanowire embedded in double-side dielectric DBRs MC [25–28]. However, from the view of electrically injected devices, QWs structure should be more suitable for low threshold laser diodes (LDs). Among GaN based QWs structure, the AlGaIn/GaN QWs were considered to be more appropriate than InGaIn/GaN QWs due to its lower inhomogeneous broadening [29]. Unfortunately, the p-type doping AlGaIn was difficult with increasing the Al content because of the inferior crystalline quality and difficulty in p-type doping of AlGaIn [30], InGaIn/GaN QWs seems to be a better choice for electrical injected polariton device. However, large inhomogeneous broadening due to the composition fluctuation in InGaIn QWs was detrimental to the strong coupling [31]. It was anticipated that exciton polariton in InGaIn/GaN QWs can only be observed under small inhomogeneous broadening and a MC based on double-side dielectric DBRs [32].

The cavity polariton and electrically pumped InGaIn-based exciton polariton light emitting diodes have been demonstrated at room temperature by Tawara and Lu, respectively [33, 34]. The exciton polariton with giant Rabi splitting in GaN/InGaIn core-shell wire and resonant reflection and suppressed absorption in periodic systems of InGaIn QWs have also been reported, respectively [35, 36]. In this paper, exciton polariton due to strong coupling between exciton and cavity photon in InGaIn MC was reported. We fabricated 4 λ MC, which consisted of InGaIn/GaN coupled QWs active layers and high-quality MC based on double dielectric DBRs. An anti-crossing behavior of strong exciton-photon coupling was observed by angle resolved PL spectra at room temperature. Our Rabi splitting energy from 40 meV–130 meV dependent on the excitation power was confirmed to be larger than any other results in InGaIn thin film F-P MC systems [20, 28, 34].

The epilayer used in this work was grown by metal organic chemical vapor deposition on sapphire substrate, included low temperature nucleation layer, 2 μ m u-GaN buffer layer and 3 μ m n-GaN layer, followed by QWs and 200 nm p-GaN (figure 1(a)). The QWs consisted of five periods of 4 nm GaN/4 nm InGaIn. On the surface of the epilayers, 16.5 pairs of SiO₂/TiO₂ DBR was first evaporated by E-beam apparatus (figure 1(b)). Then the structure was bonded to a quartz substrate (figure 1(c)), followed by the laser lift-off of sapphire (figure 1(d)). Then, chemical mechanical polishing (CMP) was used to grind the u-GaN and achieve the designed cavity thickness (figure 1(e)). The MC was accomplished by depositing top DBR (figure 1(f)). Before depositing the top DBR, we performed the atomic force microscope (AFM) on the surface of polished sample. Reflective interference was used to measure cavity length. The root mean square (RMS) roughness of the surface was 0.1 nm. The sub nano-scale surface smoothness of 0.1 nm provided the conditions for the growth of highly reflective DBRs, hence guaranteed the high quality MC.

The properties of InGaIn QWs were investigated by PL. Figure 2(a) shows the PL spectra at low temperature (13 k) and room temperature (300 k), corresponding to 3.048 eV and 3.032 eV peak energy respectively. It is noted that low temperature full width at half maximum (FWHM) was dominated by inhomogeneous broadening. In this work, the inhomogeneous broadening was about 38 meV, which satisfied the requirement of

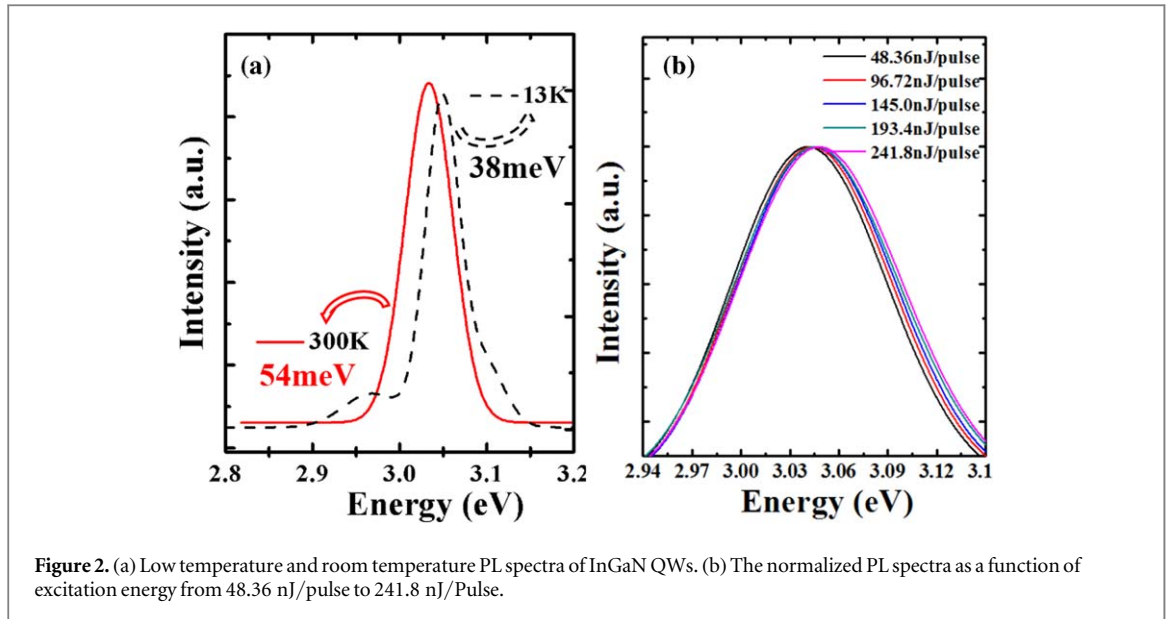


Figure 2. (a) Low temperature and room temperature PL spectra of InGaN QWs. (b) The normalized PL spectra as a function of excitation energy from 48.36 nJ/pulse to 241.8 nJ/Pulse.

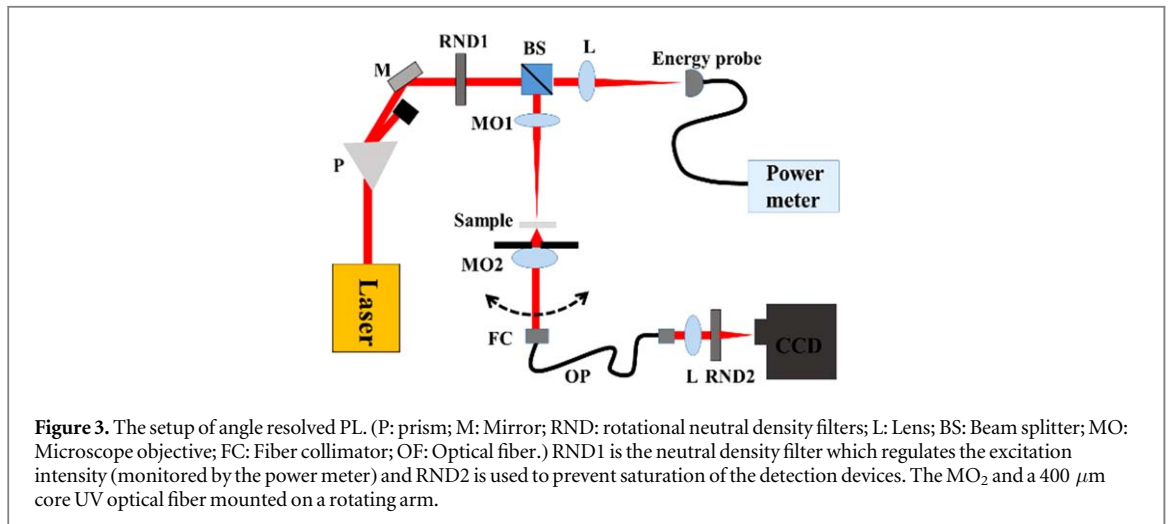
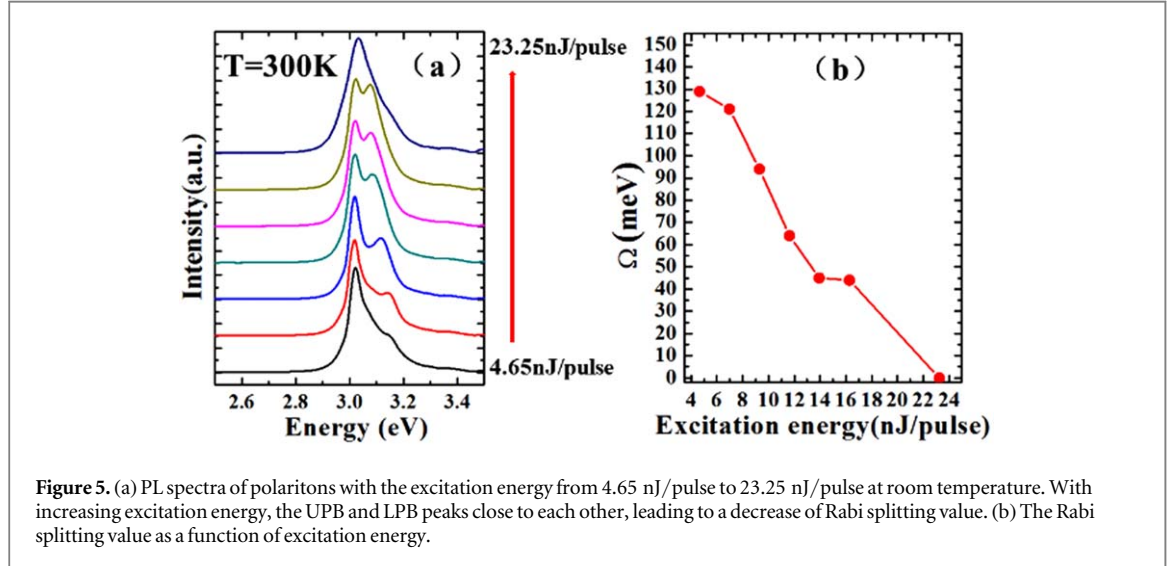
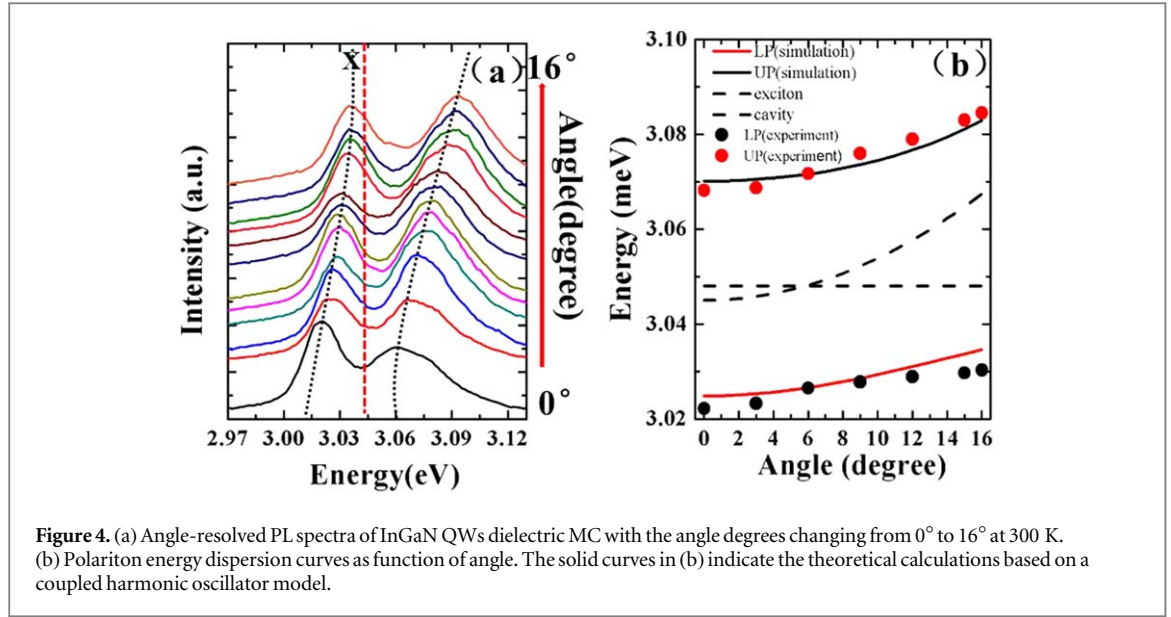


Figure 3. The setup of angle resolved PL. (P: prism; M: Mirror; RND: rotational neutral density filters; L: Lens; BS: Beam splitter; MO: Microscope objective; FC: Fiber collimator; OF: Optical fiber.) RND1 is the neutral density filter which regulates the excitation intensity (monitored by the power meter) and RND2 is used to prevent saturation of the detection devices. The MO₂ and a 400 μm core UV optical fiber mounted on a rotating arm.

strong coupling [32]. The linewidth of the PL spectrum at room temperature was 54 meV, which convolution homogeneous broadening and inhomogeneous broadening. The oscillator strength (f) is another key parameter that is necessary to achieve the strong coupling. However, f in the InGaN QWs is usually strongly reduced by quantum confined Stark effect (QCSE) resulting from both spontaneous and piezoelectric polarizations. With increasing excitation energy, we observed a tiny blue shift with the linewidth broadening at the high-energy side (figure 2(b)). This observation indicated negligible QCSE and the existence of band-filling effect [37, 38]. Calculated by the envelope function approximation, the oscillator strength was about $1.33 \times 10^{13} \text{ cm}^{-2}$, which is about three times larger than GaAs QWs exciton [4].

We measured the room temperature angle-resolved PL to investigate the characteristic of cavity polaritons with the experiment set-up shown in figure 3. The Nd:YAG 355 nm excitation source was incident on the rear of the sample with 50 Hz frequency, maximum 300 $\mu\text{J}/\text{pulse}$ excitation energy and 20 ns pulse width. The spot size of the laser focused by $50 \times$ UV microscope objective was about 10 μm . The angle-resolved PL information was collected by an objective lens and optical fiber located on a rotational unit.

Figure 4(a) shows the angle resolved PL spectrums under the excitation power of 13 nJ/Pulse. The dash lines represent free exciton energy of InGaN QWs epilayer. Two emission bands near the free exciton were clearly observed in this spectrum. As the detection angle increased, the two peaks appeared to have an anti-crossing behavior due to strong coupling between the QW excitons and cavity photons. Plotting the peak energies of the two peaks as function of angles, we obtained energy momentum dispersion curves (figure 4(b)). The figure shows that the experimental results (dots) agreed well with the theoretical calculation by coupled harmonic oscillator models (solid line):



$$E_{LP,UP}(k_{//}) = \frac{1}{2}[E_{exc} + E_{cav} \pm \sqrt{\Omega^2 + (E_{exc} + E_{cav})^2}] \quad (1)$$

where E_{exc} and E_{cav} represent the energy of excitons and photons respectively. Ω is the Rabi splitting value. This confirmed that the two emission peaks were LPB and UPB of polariton luminescence, respectively. The detuning value, defined by the difference between cavity photon and exciton energy, plays an important role in determining the energy dispersions of two polariton branches and portions of exciton and photons in polaritons [34]. In our case, the detuning was -3.0 meV at zero detection degree, where the cavity photon and exciton energy are 3.045 eV and 3.048 eV, respectively, yields 46.67% exciton portion in LPB at $k = 0$. Rabi splitting value represents the coupling strength between cavity photon and exciton in a MC. In our sample, the Rabi splitting value of 45 meV was deduced.

In order to understand the relaxation process of exciton polariton, we further measured the polariton emission spectra at different excitation energy with a fixed detection angle of 6° at room temperature. At this angle, the detuning value was close to zero. The PL spectra as function of excitation energy from 4.65 nJ/pulse to 23.25 nJ/pulse were shown in figure 5(a). At low excitation energy, two resolved polariton peaks with large splitting value of 130 meV were observed. Whereas, the two peaks progressively merged into a single emission peak as the excitation energy increased, the Rabi splitting value decreased to 40 meV with the increase of excitation energy (figure 5(b)), which was caused by increase of the exciton homogeneous broadening originating from the exciton-exciton scattering [28]. The scattering is known to increase and deteriorate exciton linewidth and coupling strength, respectively, and finally reduce the Rabi splitting value. Therefore, increasing

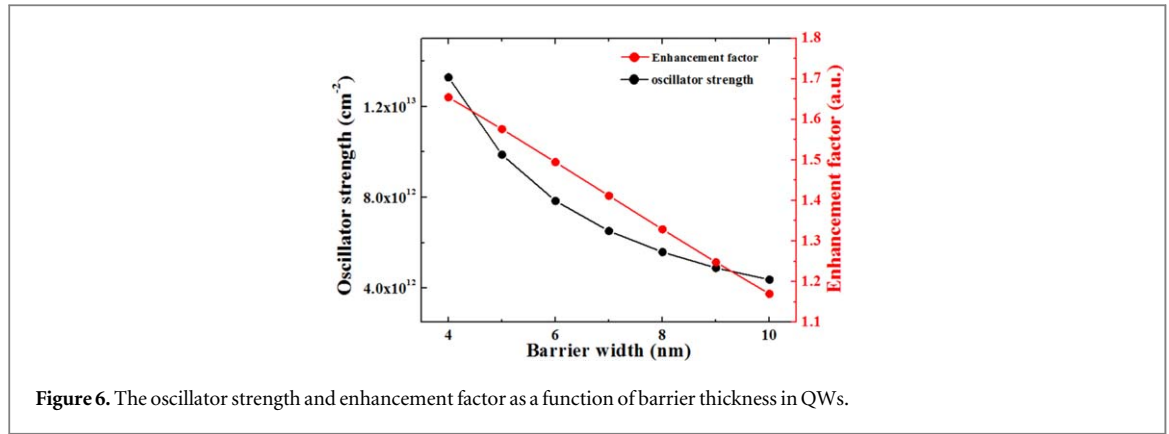


Figure 6. The oscillator strength and enhancement factor as a function of barrier thickness in QWs.

further the excitation energy leads to the disappearance of the Rabi splitting indicating a transition from strong to weak coupling.

Strong coupling with large Rabi splitting value is essential to exciton polariton device application and research on fundamental physical phenomena. In our sample, the large Rabi splitting observed was attributed to the coupled QWs structures and extremely high Q factors of our F-P cavity. The relationship between the exciton density and Rabi splitting value (Ω) is given by equation (2) [34]:

$$\Omega = 2\hbar \sqrt{g(N, L_{eff})^2 - \left(\frac{\gamma_{ex} - \gamma_{ph}}{4}\right)^2} \quad (2)$$

where γ_{ex} and γ_{ph} represent the luminescence linewidth of excitons and photons, respectively. $g(N, L_{eff})$ is a coupling factor related to the oscillator density coupled with cavity mode and L_{eff} is the effective cavity length. The coupling factor is given by [39]:

$$g(N, L) = \left[\frac{2\pi}{\epsilon_r} \frac{1}{4\pi\epsilon_0} \frac{e^2 N f}{m L_{eff}} \right]^{1/2} \quad (3)$$

where ϵ_r (ϵ_0) is the relative (vacuum) permittivity, e is the electron charge, m is the electron mass, f is the exciton oscillator strength, N is the oscillator density coupled to the cavity mode. It can be seen that the Rabi splitting value can be increased by increasing exciton oscillator (f) and the exciton density coupled to the cavity mode (N). In our experiment, a coupled QWs structure was utilized as active regions. Calculation indicates that the oscillator strength decreases with increasing the thickness of barrier in QWs (figure 6). The oscillator strength of our coupled QWs (4 nm/4 nm) is $1.33 \times 10^{13} \text{ cm}^{-2}$ per QW, and the coupled QWs transfer to the uncoupled as the barrier width increases to 10 nm, the oscillator strength is $4.37 \times 10^{12} \text{ cm}^{-2}$ in uncoupled QWs. The oscillator strength of coupled QWs excitons is about three times larger than the one of uncoupled QWs excitons. Moreover, the thin barrier layer in the coupled QWs can not only increases the oscillator strength, but also enhances the density of exciton (N) coupled to the cavity mode. The optical confinement factor describes the coupling strength between the QWs and optical field. Inserting the QWs located at the antinode of optical field, the optical confinement factor can be expressed as [40]:

$$\Gamma = \Gamma_z = \frac{L_a}{L_c} \left(1 + \frac{\sin k_z L_a}{k_z L_a} \right) \quad (4)$$

where Γ_z is the axial confinement factor, L_c is the cavity length and L_a is the thickness of QWs. The parts in the bracket can be defined as enhancement factor (ξ), which can be expressed as:

$$\xi = 1 + \sin k_z L_a / k_z L_a \quad (5)$$

In this study, five pairs coupled QWs were used as the active layer in the MC. Therefore, $\xi = 1.7$ could be achieved, showing a more effective coupling between the QWs and internal optical field. For comparison, the enhancement factor was calculated to be one in the uncoupled QWs (10 nm barriers). The higher optical confinement factor increased the possibility of interaction between photons and excitons, reflecting more excitons coupled to the cavity mode. The results indicate that the coupled QWs can greatly improve the Rabi splitting value.

Secondly, we adopted high-Q F-P cavities in our structure. Compared with the state-of-the-art $Q < 1000$, a Q value exceeding 3500 was observed in our previous samples with identical fabrication process in our previous work [41]. The MC used the double-side dielectric DBRs, where the DBRs can be deposited easily by electron beam evaporation and yield extra-high reflectivity ($>99.9\%$). The effective cavity length is 4λ , which reduces the single round trip absorption of light, hence can improve the Q value. Atomic force microscopy (AFM) scans

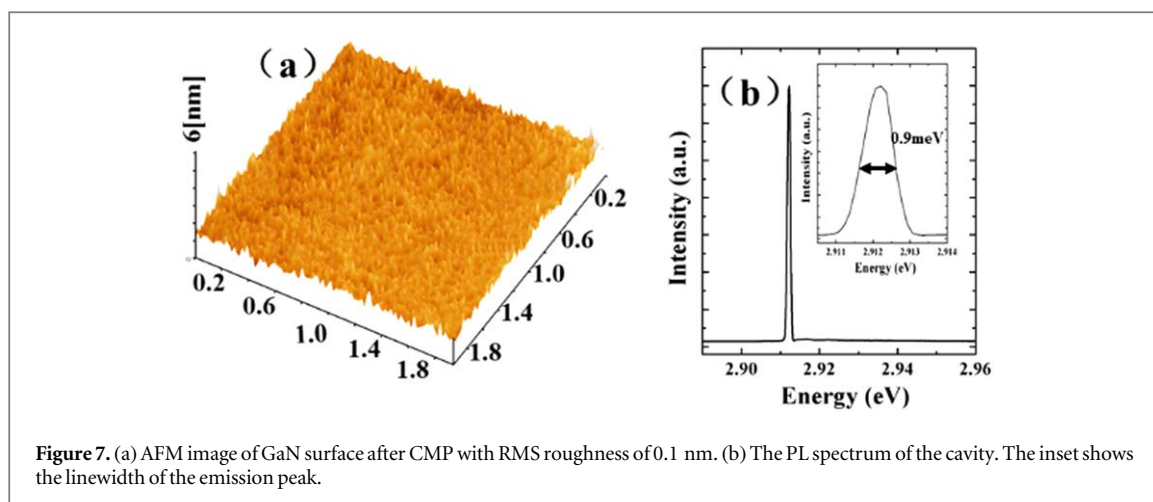


Figure 7. (a) AFM image of GaN surface after CMP with RMS roughness of 0.1 nm. (b) The PL spectrum of the cavity. The inset shows the linewidth of the emission peak.

indicated a root mean square (RMS) roughness of about 0.1 nm in a scan area of $2\ \mu\text{m} \times 2\ \mu\text{m}$ after CMP, as shown in figure 7(a). The sub-nanometer level surface roughness not only provides the conditions for the growth of highly reflective DBRs, but also reduces the scattering loss to 0.001%. For normal incidence, the scatter loss from a slightly roughened surface is approximated as [42]:

$$S_{\text{scatter}} = A\{1 - \exp[-(4\pi\delta/\lambda)^2]\} \quad (6)$$

where δ is the RMS surface roughness, λ is the operating wavelength, A is correction factor calculated here to be 1.02 according to the ratio between the total reflectance of the top DBR versus air and that versus GaN. The above factors play important roles in improving the Q value of MC. It should be noted that, a high Q value of a cavity yields a longer photon lifetime and higher possibility of strong coupling with excitons. In our work therefore, the Q value of the MC was about 3230, as shown in figure 7(b).

In conclusion, strong exciton photon coupling at room temperature has been demonstrated in a InGaN/GaN QWs MC, confirmed by the anti-cross behavior observed in the angle resolved PL. The inhomogeneous broadening and oscillator strength were 38 meV and $1.33 \times 10^{13}\ \text{cm}^{-2}$ respectively in the coupled InGaN/GaN QWs. Rabi splitting value of 40 meV–130 meV was contributed by our high Q cavity and coupled QWs structures. From the PL spectra at different excitation fluence, it was shown that the Rabi splitting energy decreased by increasing the excitation power, which was induced by the exciton-exciton scattering effect. Large Rabi splitting indicated stronger coupling and robust polaritons, which would benefit the room temperature polariton devices, including polaritonic LED, polaritonic lasing and polaritonic transportation devices. These results open a new way to study the exciton polariton and also reveal that the MCs based on dielectric DBRs are promising candidates for practical polariton devices.

Acknowledgments

This work was supported by the National Key Research and Development Program of China (No. 2016YFB0400803), the Science Challenge Project (No. TZ2016003), the National Natural Science Foundation of China (Nos. 61704140, U1505253).

ORCID iDs

Hao Long  <https://orcid.org/0000-0002-7057-7214>

BaoPing Zhang  <https://orcid.org/0000-0001-9537-5179>

References

- [1] Weisbuch C, Nishioka M, Ishikawa A and Arakawa Y 1992 *Phys. Rev. Lett.* **69** 3314
- [2] Imamoglu A, Ram R J, Pau S and Yamamoto Y 1996 *Phys. Rev. A* **53** 4250
- [3] Senellart P and Bloch J 1999 *Phys. Rev. Lett.* **82** 1233
- [4] Houdre R, Weisbuch C, Stanley R P, Oesterle U, Pellandini P and Ilegems M 1994 *Phys. Rev. Lett.* **73** 2043
- [5] Kerry Vahala J 2003 Optical microcavities *Nature* **424** 839–46
- [6] Kasprzak J et al 2006 *Nature* **443** 409
- [7] Balili R, Hartwell V, Snoke D, Pfeiffer L and West K 2007 *Science* **316** 1007
- [8] Bhattacharya P, Frost T, Deshpande S, Baten M Z, Hazari A and Das A 2014 *Phys. Rev. Lett.* **112** 236802

- [9] Heo J, Jahangir S, Xiao B and Bhattacharya P 2013 *Nano Lett.* **13** 2376
- [10] Savvidis P G, Baumberg J J, Stevenson R M, Skolnick M S, Whittaker D M and Roberts J S 2000 *Phys. Rev. Lett.* **84** 1547
- [11] Saba M *et al* 2001 *Nature* **414** 731
- [12] El-Bakkari K, Sali A, Iqraoun E, Rezzouk A, Es-Sbai N and Ouazzani Jamil M 2018 *Physica B: Condensed Matter* **538** 85–94
- [13] Malpuech G, Di Carlo A, Kavokin A, Baumeberg J J, Zamfirescu M and Lugli P 2002 *Appl. Phys. Lett.* **81** 412
- [14] Bajoni D, Senellart P, Wertz E, Sagnes I, Miard A, Lemaitre A and Bloch J 2008 *Phys. Rev. Lett.* **100** 047401
- [15] Tsintzos S I, Pelekanos N T, Konstantinidis G, Hatzopoulos Z and Savvidis P G 2008 *Nature* **453** 06979
- [16] Khalifa A A, Love A P D, Krizhanovskii D N, Skolnick M S and Roberts J S 2008 *Appl. Phys. Lett.* **92** 061107
- [17] Bajoni D, Semenova E, Lemaitre A, Bouchoule S, Wertz E, Senellart P and Bloch J 2008 *Phys. Rev. B* **77** 113303
- [18] Bhattacharya P, Xiao B, Das A, Bhowmick S and Heo J 2013 *Phys. Rev. Lett.* **110** 206403
- [19] Baten M Z, Bhattacharya P, Frost T, Deshpande S, Das A, Lubyshev D, Fastenau J M and Liu A W K 2014 *Appl. Phys. Lett.* **104** 231119
- [20] Christmann G, Butté R, Feltin E, Mouti A, Stadelmann P A, Castiglia A, Carlin J-F and Grandjean N 2008 *Phys. Rev. B* **77** 085310
- [21] Kornitzer K, Ebner T, Thonke K and Sauer R 1999 *Phys. Rev. B* **60** 1471–3
- [22] Özgür Ü, Bergmann M J, Casey H C Jr, Everitt H O, Abare A C, Keller S and DenBaars S P 2000 *Appl. Phys. Lett.* **77** 109
- [23] Butté R, Christmann G, Feltin E, Carlin J-F, Mosca M, Illegems M and Grandjean N 2006 *Phys. Rev. B* **73** 033315
- [24] Semon F, Sellers I R, Natali F, Byrne D, Leroux M, Massies J, Ollier N, Leymarie J, Disseix P and Vasson A 2005 *Appl. Phys. Lett.* **87** 021102
- [25] Bhattacharya A, Baten M Z, Iorsh I, Frost T, Kavokin A and Bhattacharya P 2017 *Phys. Rev. Lett.* **119** 067701
- [26] Bhattacharya P, Frost T, Deshpande S, Baten M Z, Hazari A and Das A 2014 *Phys. Rev. Lett.* **112** 236802
- [27] Junseok Heo S, Jahangir B, Xiao B and Bhattacharya P 2013 *Nano Lett.* **13** 2376
- [28] Das A, Heo J, Jankowski M, Guo W, Zhang L, Deng H and Bhattacharya P 2011 *Phys. Rev. Lett.* **107** 066405
- [29] Christmann G, Butté R, Feltin E, Carlin J-F and Grandjean N 2008 *Appl. Phys. Lett.* **93** 051102
- [30] Suzuki M, Nishio J, Onomura M and Hongo C 1998 *J. Cryst. Growth* **189–190** 511
- [31] Christmann G, Butté R, Feltin E, Carlin J-F and Grandjean N 2008 *Phys. Rev. B* **73** 153305
- [32] Glauser M, Mounir C, Rossbach G, Feltin E, Carlin J-F, Butté R and Grandjean N 2014 *J. Appl. Phys.* **115** 233511
- [33] Lu T-C, Chen J-R, Lin S C, Huang S-W, Wang S C and Yamamoto Y 2011 *Nano Lett.* **11** 2791
- [34] Tawara T, Gotoh H, Akasaka T, Kobayashi N and Saitoh T 2004 *Phys. Rev. Lett.* **92** 256402
- [35] Gong S-H, Ko S-M, Jang M-H and Cho Y-H 2015 *Nano Lett.* **15** 4517–24
- [36] Bolshakov A S, Chaldyshev V V, Zavarin E E, Sakharov A V, Lundin W V, Tsatsulnikov A F and Yagovkina M A 2017 *J. Appl. Phys.* **121** 133101
- [37] Grandjean N, Damilano B, Dalmaso S, Leroux M, Laugt M and Massies J 1999 *J. Appl. Phys.* **86** 3714–0
- [38] Leroux M *et al* 1998 *Phys. Rev. B* **58** R13371–4
- [39] Andreani L C, Panzarini G and Gerard J M 1999 *Phys. Rev. B* **60** 13276
- [40] Colclough L A and Corzine S W 2006 *Diode Lasers and Photonic Integrated Circuits* (Beijing, China: Beijing University of Posts and Telecommunications) 341
- [41] Liu W J, Hu X L, Ying L Y, Zhang J Y and Zhang B P 2014 *Appl. Phys. Lett.* **104** 251116
- [42] Guenther K H, Wierer P G and Bennett J M 1984 *Appl. Opt.* **23** 3820